# Superradiant terahertz emission by dipolaritons

O. Kyriienko,[1,2] A. V. Kavokin,[3,4] and I. A. Shelykh[1,2]

[1]*Science Institute, University of Iceland, Dunhagi-3, IS-107, Reykjavik, Iceland*
[2]*Division of Physics and Applied Physics, Nanyang Technological University 637371, Singapore*
[3]*School of Physics and Astronomy, University of Southampton, Highfield, Southampton SO17 1BJ, United Kingdom*
[4]*Spin Optics Laboratory, St. Petersburg State University, 1, Ulianovskaya, 198504, Russia*

(Dated: January 31, 2013)

Dipolaritons are mixed light-matter quasiparticles formed in double quantum wells embedded in microcavities. Due to resonant coupling between direct and indirect excitons via electronic tunnelling, dipolaritons possess large dipole moments. Resonant excitation of the cavity mode by a short pulse of light induces oscillations of the indirect exciton density with a characteristic frequency of Rabi flopping. This results in oscillations of classical Hertz dipoles array which generate supperradiant emission on a terahertz (THz) frequency. Resulting THz signal may be enhanced using the supplementary THz cavity in the weak coupling regime.

*Introduction.* Generation and frequency modulation of terahertz radiation is one of major technological challenges nowadays [1]. Applications of terahertz sources span from communication technologies to medicine and security. The existing THz emitters are based on a large variety of physical principles [2]. One possible solution is a conventional solid state oscillator based on a high frequency Gunn or tunnelling diode [3]. The operating frequency of such oscillator is limited to the microwave region and the lower boundary of terahertz range. Second, quantum cascade lasers (QCL) allow for coherent emission of radiation in a terahertz range [4, 5]. Exploiting the multiple photon emission from intersubband transition of wide quantum wells [6], QCL cover the upper boundary of THz range with relatively high power of emission (up to 50 mW). QCL operate at cryogenic temperatures which strongly limits their application area. The laser driven terahertz emitters form a third group of THz sources, where femtosecond optical pulse illuminating the semiconductor structure leads to oscillation of carrier density which generates terahertz radiation [7–9]. Similar effects can be observed in crystals with a large second-order susceptibility where time-varying polarization induces THz emission [10]. Finally, the wide group of THz emitters are free electron based sources like klystron or free electron laser. These are powerful but quite bulky sources. Optimization of spectral characteristics, size, efficiency, cost and operation temperature of terahertz sources is one of the priority objectives of modern optoelectronics. Here we propose a compact optical to terahertz radiation convertor allowing for efficient frequency modulation and operating at high temperatures.

Theoretical proposals for THz sources in solid state and semiconductor physics present a rich diversity. One example is the use of carbon nanostructures, in particular, carbon nanotubes (CNT's) [11, 12], or Aharonov-Bohm quantum rings [13]. Another area where a possibility of THz generation has been widely studied theoretically is *polaritonics* — the interdisciplinary research area at the boundary of solid state physics and quantum optics [6, 15]. Polaritonic devices are based on the strong coupling between excitons in semiconductor quantum wells and confined photons. Proposals include the polariton based THz emitters where signal is generated from transitions between upper and lower polariton branches [1, 16, 18] and transition between $2p$ and $1s$ exciton states, the latter one strongly coupled to the cavity mode [2]. Recent theoretical studies also include the proposal of bosonic cascade lasers realized due to the multiple THz photon emission by excitons (exciton-polaritons) confined in a parabolic potential trap [20]. Our present proposal is based on the recent experimental realization of dipolaritons — cavity exciton-polaritons characterized by large dipole moments.

The mechanism for terahertz signal generation described in this Letter relies on the beats between spatially direct and indirect excitons. Spatially indirect excitons are composed of electrons and holes situated in separate quantum wells (QWs) [21]. Coupled QW systems where separation of electrons and holes and energy splitting between direct and indirect excitons can be controlled by applied electric fields have been studied in the recent decades [22–24]. The radiative lifetimes of indirect excitons are usually much longer than those of direct excitons due to the lower electron–hole overlap. Another important feature of indirect excitons is their large dipole moments in the normal to QW plane direction resulting in strong exciton-exciton interactions [25].

Recently, it has been shown that exciton polaritons and spatially indirect excitons can be intermixed in the biased semiconductor microcavities with embedded coupled QWs [7, 8, 26]. In these structures new quasiparticles being linear superposition of cavity photon (C), direct exciton (DX) and indirect exciton (IX) appear. They form three exciton-polariton modes, namely, the upper polariton (UP), middle polariton (MP) and lower polariton (LP) modes. These modes may be characterized by large dipole moments which is why they are referred to

as *dipolaritons* [8].

Here we study theoretically the effect of beats between dipolariton modes due to the tunnel coupling between direct and indirect excitons. The combined tunnelling and cavity-exciton coupling effects result in Rabi flopping between two dipolariton modes and lead to harmonic oscillations of IX density. Since indirect excitons represent elementary dipoles, these density oscillations result in emission of THz frequency radiation whose characteristics can be tuned by the applied bias and pumping conditions. This mechanism of THz radiation is similar to downshift optical-to-THz frequency conversion used in laser driven terahertz emitters and allows for high power generation. The essential difference of the generation scheme we propose from the previously studied schemes is in the use of the superradiance effect appearing due to the fact that Rabi oscillations in the dipolariton system are coherent. Rabi oscillations can be sustained by the cavity for several tens of picoseconds. This strongly improves the quantum efficiency of the emitter.

*The model.* The structure we consider represents two QWs separated by a barrier which is sufficiently thin to allow for resonant electron tunnelling (Fig. 1). The electron wave function is shared between two QWs in this case. The optical microcavity is tuned to the wider QW exciton resonance (the left QW in Fig. 1), while the right QW remains decoupled from the optical pump. Pulsed pumping creates electron-hole pairs which form direct excitons. The bias applied in growth direction induces mixing of direct and indirect exciton states. Coupling of the cavity photons to direct excitons resulting in appearance of two polariton modes has been extensively studied [6, 15]. The coupling and anticrossing of DX-IX resonances tuned by electric field is also a well-known effect in GaAs/AlGaAs QW structures [29, 30]. Both effects combined result in the appearance of dipolaritons studied recently by Cristofolini *et al.* [8].

The correct treatment of a real dipolariton system should in principle involve both coherent and decoherent parts for the Hamiltonian, $\hat{H} = \hat{H}_{coh} + \hat{H}_{dec}$. The Hamiltonian corresponding to the coherent part reads

$$\hat{\mathcal{H}}_{coh} = \hbar\omega_C \hat{a}^\dagger \hat{a} + \hbar\omega_{DX} \hat{b}^\dagger \hat{b} + \hbar\omega_{IX} \hat{c}^\dagger \hat{c} + \frac{\hbar\Omega}{2}(\hat{a}^\dagger \hat{b} + \hat{b}^\dagger \hat{a}) - \frac{\hbar J}{2}(\hat{b}^\dagger \hat{c} + \hat{c}^\dagger \hat{b}) + P\hat{a}^\dagger + P^* \hat{a}, \tag{1}$$

where $\hat{a}^\dagger$, $\hat{a}$, $\hat{b}^\dagger$, $\hat{b}$ and $\hat{c}^\dagger$, $\hat{c}$ are creation and annihilation operators for cavity photons, direct excitons and indirect excitons, respectively. Here $\hbar\omega_C$, $\hbar\omega_{DX}$ and $\hbar\omega_{IX}$ denote cavity mode, direct exciton and indirect exciton energies, and first three terms of Hamiltonian describe energy of bare modes. The fourth and fifth terms correspond to coupling between modes, where $\hbar\Omega$ (Rabi splitting) [32] denotes the coupling constant between photon and direct exciton, and the tunnelling rate corresponding to DX–IX coupling is $\hbar J$. The last two terms in Hamiltonian correspond to the optical pumping of cavity mode with rate $P(t) = P_0(t)e^{i\omega_P t}$, where $\omega_P$ is a pumping frequency. In the following considerations we omit summation over space indices since we are mostly interested in temporal dynamics of the system. The decoherent part of Hamiltonian $\hat{\mathcal{H}}_{dec}$ in general can contain the terms corresponding to different dissipative processes, including finite lifetimes of the modes and pure decoherence. The dynamics of the system can be calculated from Master equation for the density matrix,

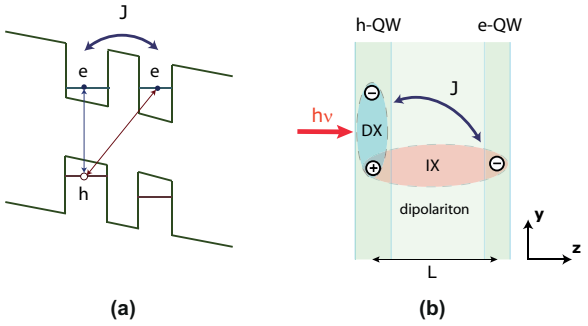


FIG. 1: (Color online) Sketch of the system. (a) Double quantum well (DQW) heterostructure with resonantly coupled electron levels and a hole in the left quantum well (QW). The right QW has larger bandgap than left QW tuned by the presence of indium alloy or width of the well. (b) Electron-hole bilayer with schematic picture of coupled spatially indirect and direct exciton which form dipolariton.

$$i\hbar\frac{\partial\rho}{\partial t} = [\hat{\mathcal{H}}_{coh}, \rho] + \hat{\mathcal{L}}\rho, \tag{2}$$

where $\hat{\mathcal{L}}$ denotes a Linblad superoperator responsible for accounting of incoherent processes [1, 2]. Its detailed form is given in Supplementary material, section A [31].

In the following Letter we are interested in the large occupation numbers of the modes, and mean-field approximation is eligible. The dynamics of occupation numbers of the modes can be found from the Master equation (2), where operators are treated as classical fields [the details of this derivation are given the Supplementary Material, section A]

$$\frac{\partial\langle\hat{a}\rangle}{\partial t} = -i\frac{\Omega}{2}\langle\hat{b}\rangle - \frac{\gamma_C}{2}\langle\hat{a}\rangle - i\widetilde{P}, \tag{3}$$

$$\frac{\partial\langle\hat{b}\rangle}{\partial t} = i\delta_\Omega\langle\hat{b}\rangle - i\frac{J}{2}\langle\hat{c}\rangle - i\frac{\Omega}{2}\langle\hat{a}\rangle - \frac{\gamma_{DX}}{2}\langle\hat{b}\rangle, \tag{4}$$

$$\frac{\partial\langle\hat{c}\rangle}{\partial t} = i(\delta_\Omega - \delta_J)\langle\hat{c}\rangle - i\frac{J}{2}\langle\hat{b}\rangle - \frac{\gamma_{IX}}{2}\langle\hat{c}\rangle, \tag{5}$$

where $\langle ... \rangle = \mathrm{Tr}\{...\rho\}$ denotes averaging using the density matrix $\rho$, and occupation numbers for modes can be found as $n_C = \langle\hat{a}\rangle\langle\hat{a}\rangle^*$, $n_{DX} = \langle\hat{b}\rangle\langle\hat{b}\rangle^*$ and $n_{IX} = \langle\hat{c}\rangle\langle\hat{c}\rangle^*$. Here we applied the rotating wave approximation $\langle\hat{a}_i\rangle \rightarrow$

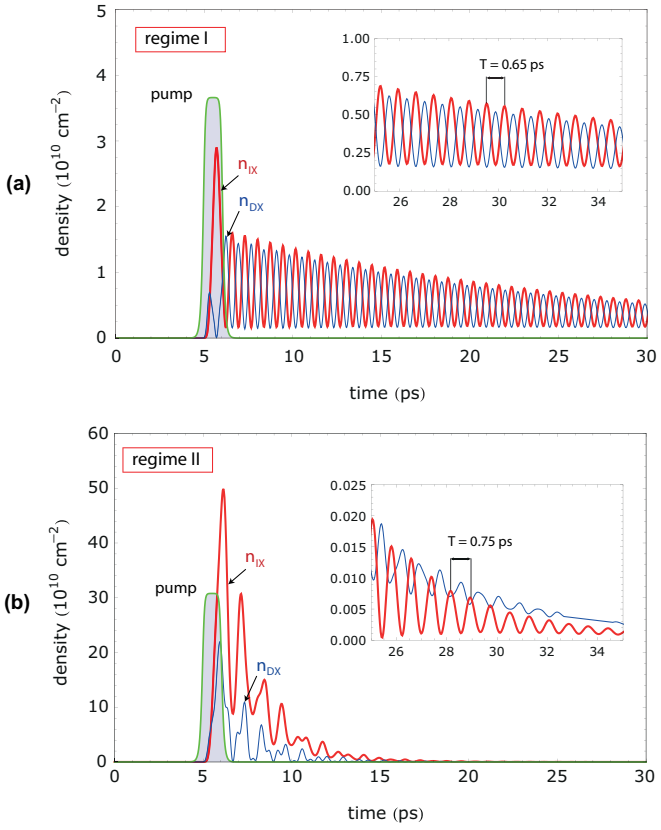


FIG. 2: (Color online) Dynamics of the dipolariton system subjected to pulsed optical pumping which shows oscillations of indirect exciton (red line, $n_{IX}$) and direct exciton (blue line, $n_{DX}$) density. The coupling constants are equal to $\hbar J = \hbar\Omega = 6$ meV. (a) Oscillations of density in regime I, where cavity mode is detuned from direct exciton resonance by $\delta_\Omega = -10$ meV. Pumping frequency is chosen as $\hbar\Delta = 11.5$ meV, and we plot oscillations for electric field $F = 0.95F_0$, where $F_0$ is field corresponding to IX-DX resonance (e.g. $F_0 = 12.5$ kV/cm in Ref. [7]). The green area schematically represents optical pulse with duration $\Delta\tau = 1$ ps and pulse edge defined by 0.1 ps transient time (pump, scaled intensity). The inset shows the long-term term oscillations of $n_{IX}(t)$ and $n_{DX}(t)$ density which are in antiphase. The period of oscillations is equal to $T = 0.65$ ps. (b) Oscillations corresponding to regime II, where detuning is equal to $\delta_\Omega = 3$ meV. For the same electrical field and pump intensity ($\hbar\Delta = 0$) the magnitude of signal is higher comparing to regime I. Inset shows highly damped long-term oscillations in the second regime.

$\langle\hat{a}_i\rangle e^{-i\omega_C t}$, and introduced the photonic $\delta_\Omega = \omega_C - \omega_{DX}$ and excitonic $\delta_J = \omega_{IX} - \omega_{DX}$ detunings. The pumping rate reads as $\tilde{P}(t) = P_0(t)e^{-i\Delta t}$, where $\Delta = \omega_P - \omega_C$ denotes detuning of the coherent optical pumping. The damping rates of the modes are defined by parameters $\gamma_i = 2\pi/\tau_i$, $i = C,\ DX,\ IX$. Typical lifetimes of the modes are $\tau_C \approx 3$ ps, $\tau_{DX} \approx 1$ ns and $\tau_{IX} \approx 100$ ns.

Additionally, we derived dynamic equations for occupation numbers for the modes going to higher order of mean-field theory and verified validity of the system (34)–(36) for chosen pumping conditions. The former model represents the general description of dipolariton system and allows for accounting of various decoherent processes including pure dephasing [see Supplementary information, section B].

*Results and discussion.* We calculate numerically the dynamics of the system with coupled quasiparticles subjected to a picosecond pulsed optical pumping. The presence of mixing terms between different modes implies the oscillating behavior similar to Rabi flopping in the classical model of a two-level system subjected to a time-varying field. It is important to note that our system has several characteristic frequencies. They are governed by the exciton-photon coupling strength $\Omega$ and detuning $\delta_\Omega$, the IX-DX coupling strengths $J$ and detuning $\delta_J$. Additionally, the pumping frequency $\omega_P$ governs the efficiency of the pump. Varying these characteristic frequencies one can control the frequency, magnitude and damping rate of indirect exciton density oscillations.

While the coupling constants $\Omega$ and $J$ are dependent on the geometry of the structure and can hardly be tuned for a given sample, the detunings between modes $\delta_J$ and $\delta_\Omega$ are strongly sensitive to the applied electric field and the incidence angle of the cavity pump [8]. Tuning these parameters one can bring the oscillating dipole system to different regimes. If the cavity mode is far-detuned from IX-DX anti-crossing the light-exciton coupling is weak, which will be referred to as the regime $I$. If the detuning $\delta_\Omega$ is small the strong intermixing of IX, DX, and C modes takes place, which corresponds to the regime $II$.

The behavior of the system in the regime $I$ is shown in Fig. 2(a) for the detuning $\delta_\Omega = -10$ meV. We observe antiphase oscillations of IX and DX densities with decaying amplitudes. The inset in Fig. 2(a) shows a zoom of long-standing phase-locked oscillations which last for several tens of picoseconds. For the electric field $F$ approximately equal to the resonant field of IX-DX modes anti-crossing $F_0$ the frequency of oscillations is given by $\nu \approx J/2\pi = 1.45$ THz. The time dependence of indirect exciton density oscillation $n_{IX}(t)$, calculated numerically from system (34)–(36), can approximately be fitted with analytical function as

$$n_{IX}(t) = n^0_{IX}\cos^2(\omega t/2)e^{-t/\tau}, \qquad (6)$$

where $\omega = 2\pi\nu$ is the frequency of oscillations, $n^0_{IX}$ denotes the magnitude of oscillations which decreases in time with the damping rate $\tau^{-1}$. Tuning the electric field, the frequency of generated oscillations changes in the range of several THz due to its dependence on IX-DX detuning (Fig. 6). Other important parameters of the system such as the amplitude of oscillations and dimensionless oscillation quality factor $\xi$ defined as ratio of magnitude to the decrement of oscillations can be tuned by variation of pumping conditions, as well as by the applied electric field [see Supplemental Material, section D, for details].

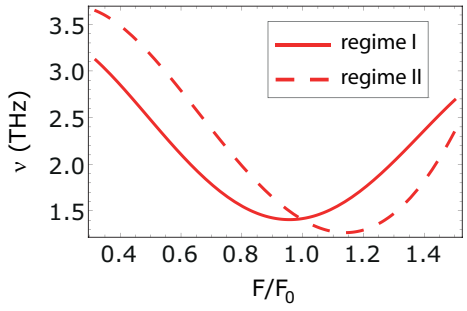


FIG. 3: (Color online) Frequency of indirect exciton density oscillations as a function of dimensionless electric field calculated for oscillations in regime I (solid line) and regime II (dashed line).

Decreasing the detuning between exciton and photon modes $\delta_\Omega$ one can bring the system into the regime $II$. In this regime the IX density oscillations are observed as well, while their quality factor is different. Strong interactions of the cavity mode with the IX-DX resonance result in a higher magnitude of $n_{IX}$ oscillations than in the regime $I$ (Fig. 2(b)). The damping rate of these oscillations is also larger. Clearly, the regime of strong coupling between all modes is advantageous for the pulsed pumping regime and it allows for high power generation. On the other hand, the regime $I$ is preferential for the long-standing signal generation providing higher quality factor $\xi$, while lower amplitude of oscillations.

We have shown that due to the coupling between modes IX and DX densities oscillate with a THz frequency. This infers that a dipolariton is an oscillating dipole, with a dipole moment in $z$ direction $d_z$ changing periodically from value $d_z = d_0$ corresponding to an indirect exciton (IX) to $d_z = 0$ corresponding to a direct exciton (DX). One can define the total dipole moment of the system as $D_z = N_{IX} d_z$, where $N_{IX} = n_{IX} A$ is the number of indirect excitons within the area $A$ illuminated by the pumping light. Since we have shown before that after initial transient regime the density of indirect excitons $n_{IX}(t)$ is decaying harmonic function of time, the total dipole moment of the system can be found as

$$D_z(t) = d_0 n_{IX} A \cos^2(\omega t/2) e^{-t/\tau}. \quad (7)$$

Here $n_{IX}$ is the maximum density of indirect excitons.

The mechanism of THz radiation by an oscillating density of indirect excitons is similar to the photo-Dember effect where oscillations of electron-hole plasma on a surface of semiconductor generate THz signal [9, 33] and other laser driven terahertz emitters. However, the system of dipolaritons has some important advantages over previously studied systems, namely: (1) the better tunability of the system allowing for fast modulation of the THz emission frequency; (2) improved spectral characteristics of THz signal which can be controlled using applied voltage and pumping conditions; (3) possibility to achieve a high output power as it is described below.

The total intensity of the far field radiation emitted by a classical Hertz dipole can be found from [34]

$$I = \frac{\ddot{D}_z^2}{6\pi\epsilon_0 c^3}, \quad (8)$$

where $D_z$ is the total dipole moment of the dipolariton array, $\epsilon_0$ is vacuum permittivity and $c$ is the speed of light. For the particular case of an array of harmonic dipole oscillations the intensity is

$$I = N_{IX}^2 \frac{d_0^2 \omega^4}{3\pi\epsilon_0 c^3}, \quad (9)$$

where $d_0 = eL$ is a dipole moment of indirect exciton with $L$ being separation between centers of QWs. Here for simplicity we did not consider the damping part $e^{-t/\tau}$ of oscillations, which can be added straightforwardly. It will result into damping of total power of emission, which is why to achieve stable cw radiation one therefore needs to use sequence of pump pulses. Similarly to the conventional case of elementary dipole emitter, the polar pattern is given by $I_\theta \sim \sin^2\theta$, where $\theta$ is an angle between direction of radiation and the axis of the structure (see Supplementary information, section E, Fig. 3).

It is important to note that total emitted intensity is proportional to the square of the density of indirect excitons and is dependent on the pump intensity in nonlinear way. This is a manifestation of the *superradiance* [35–37] effect: due to the interference of coherent in-phase oscillations of elementary dipoles the output power is enhanced. This effect is sensitive the quality factor of the cavity: the longer Rabi oscillations persist the stronger the amplification effect is. Superradiance is a specific feature of the dipolariton THz emitter, which makes it more efficient than any existing laser-to-THz convertor.

For $\hbar J = 6$ meV and the typical distance between QWs of $L = 12$ nm, the power of the THz emission of one elementary dipole formed by a dipolariton is $I_0 = 1.8\times10^{-17}$ W $= 18$ aW. The total power emitted is given by this quantity multiplied by the number of elementary dipoles $N_{IX}$. For the typical concentration of indirect excitons achievable experimentally of $n_{IX} = 10^{10}\ cm^{-2}$ and a 60 $\mu$m diameter of the pumping spot one obtains $I_{tot} \approx 1.4\ \mu$ W. By embedding a stack of double quantum wells $n_{DQW} = 4$ in each microcavity and using several sets of cavities on one chip one can obtain the output power similar to one of quantum cascade lasers.

Furthermore, to improve the efficiency of THz radiation, the system can be placed in an external cavity tuned to the THz frequency. It can be created using metallic mirrors or using an inductor capacitor circuit [6, 38]. The sketch of the system is shown in Supplementary information [section E, Fig. 3]. The efficiency of the emission would be further increased by the Purcell factor of the external cavity [6]. For the chosen frequency 1.45 THz

the experimentally achieved Purcell factor of an inductor-capacitor cavity is about $F_P = 17$ [38].

*Conclusions.* We have shown that the system of dipolaritons can provide an efficient tunable source of THz radiation. In this system, due to the direct-indirect exciton coupling, the optically excited dipolariton system exhibits density oscillations with a subpicosecond period. The dipole oscillations lead to the superradiant emission of radiation in the THz frequency range. The spectral properties as well as the power output of this system are expected to be strongly improved with respect to the existing laser induced THz emitters. Additionally, we propose a way to enhance the radiation efficiency using a supplementary THz cavity in the weak coupling regime.

This work has been supported by Rannis "Center of Excellence in Polaritonics" and FP7 IRSES project "POLATER". O. Kyriienko acknowledges the support from Eimskip Fund. We thank Sven Hofling and Jeremy Baumberg for useful discussions on the subject.

[1] P. H. Siegel, IEEE Trans. Microw. Theory Techn. **50**, 910 (2002).
[2] G. P. Gallerano and S. Biedron, in *Proceedings of the 2004 FEL Conference, Trieste, Italy, 2004*, p. 216-221.
[3] H. Eisele, IEEE Trans. Microw. Theory Techn. **48**, 626 (2000).
[4] J. Faist, F. Capasso, D. L. Sivco, C. Sirtori, A. L. Hutchinson, and A. Y. Cho, Science **264**, 553 (1994).
[5] R. Köhler, A. Tredicucci, F. Beltram, H. E. Beere, E. H. Linfield, A. G. Davies, D. A. Ritchie, R. C. Iotti, and F. Rossi, Nature **417**, 156 (2002).
[6] M. Geiser, F. Castellano, G. Scalari, M. Beck, L. Nevou, and J. Faist, Phys. Rev. Lett. **108**, 106402 (2012).
[7] D. H. Auston, K. P. Cheung, J. A. Valdmanis, and D. A. Kleinman, Phys. Rev. Lett. **53**, 1555 (1984).
[8] C. Fattinger and D. Grischkowsky, Appl. Phys. Lett. **54**, 490 (1989).
[9] J. Shan and T. F. Heinz, Topics Appl. Phys. **92**, 59 (2004).
[10] Z. Jiang and X.-C. Zhang, IEEE Trans. Microw. Theory Techn. **47**, 2644 (1999).
[11] O. V. Kibis, M. R. da Costa, and M. E. Portnoi, Nano Lett. **7**, 3414 (2007).
[12] K. G. Batrakov, O. V. Kibis, P. P. Kuzhir, M. R. da Costa, and M. E. Portnoi, J. Nanophoton. **4**, 041665 (2010).
[13] A. M. Alexeev and M. E. Portnoi, Phys. Rev. B **85**, 245419 (2012).
[14] A. V. Kavokin, J. J. Baumberg, G. Malpuech, and F. P. Laussy, *Microcavities* (Oxford University Press, Oxford, 2007).
[15] T. C. H. Liew, I. A. Shelykh, and G. Malpuech, Physica E **43**, 1543 (2011).
[16] K. V. Kavokin, M. A. Kaliteevski, R. A. Abram, A. V. Kavokin, S. Sharkova, and I. A. Shelykh, Appl. Phys. Lett. **97**, 201111 (2010).
[17] I. G. Savenko, I. A. Shelykh, and M. A. Kaliteevski, Phys. Rev. Lett. **107**, 027401 (2011).
[18] E. del Valle and A. V. Kavokin, Phys. Rev. B **83**, 193303 (2011).
[19] A. V. Kavokin, I. A. Shelykh, T. Taylor, and M. M. Glazov, Phys. Rev. Lett. **108**, 197401 (2012).
[20] T. C. H. Liew, M. M. Glazov, K. V. Kavokin, I. A. Shelykh, M. A. Kaliteevski, and A. V. Kavokin, Phys. Rev. Lett. **110**, 047402 (2013).
[21] Yu. E. Lozovik and V. I. Yudson, Sov. Phys. JETP **44**, 389 (1976).
[22] L. V. Butov, A. L. Ivanov, A. Imamoglu, P. B. Littlewood, A. A. Shashkin, V. T. Dolgopolov, K. L. Campman, and A. C. Gossard, Phys. Rev. Lett. **86**, 5608 (2001).
[23] D. Snoke, Science **298**, 1368 (2002).
[24] A. A. High, J. R. Leonard, A. T. Hammack, M. M. Fogler, L. V. Butov, A. V. Kavokin, K. L. Campman, and A. C. Gossard, Nature **483**, 584 (2012).
[25] O. Kyriienko, E. B. Magnusson, and I. A. Shelykh, Phys. Rev. B **86**, 115324 (2012).
[26] G. Christmann, C. Coulson, J. J. Baumberg, N. T. Pelekanos, Z. Hatzopoulos, S. I. Tsintzos, and P. G. Savvidis, Phys. Rev. B **82**, 113308 (2010).
[27] G. Christmann, A. Askitopoulos, G. Deligeorgis, Z. Hatzopoulos, S. I. Tsintzos, P. G. Savvidis, and J. J. Baumberg, Appl. Phys. Lett. **98**, 081111 (2011).
[28] P. Cristofolini, G. Christmann, S. I. Tsintzos, G. Deligeorgis, G. Konstantinidis, Z. Hatzopoulos, P. G. Savvidis, and J. J. Baumberg, Science **336**, 704 (2012).
[29] K. Sivalertporn, L. Mouchliadis, A. L. Ivanov, R. Philp, and E. A. Muljarov, Phys. Rev. B **85**, 045207 (2012).
[30] M. Bayer, V. B. Timofeev, F. Faller, T. Gutbrod, and A. Forchel, Phys. Rev. B **54**, 8799 (1996).
[31] Supplementary Information weblink.
[32] H. Haug and S. W. Koch, *Quantum Theory of the Optical and Electronic Properties of Semiconductors* (World Scientific, Singapore, 1990).
[33] M. B. Johnston, D. M. Whittaker, A. Corchia, A. G. Davies, and E. H. Linfield, Phys. Rev. B **65**, 165301 (2002).
[34] L. D. Landau and E. M. Lifshitz, *The Classical Theory of Fields* (Butterworth-Heinemann, 1980).
[35] R. H. Dicke, Phys. Rev. **93**, 99 (1954).
[36] J. G. Bohnet, Z. Chen, J. M. Weiner, D. Meiser, M. J. Holland, and J. K. Thompson, Nature **484**, 7392 (2012).
[37] V. I. Yukalov and E. P. Yukalova, Phys. Rev. B **81**, 075308 (2010).
[38] C. Walther, G. Scalari, M. I. Amanti, M. Beck, and J. Faist, Science **327**, 1495 (2010).

## Supplemental Material: Superradiant terahertz emission by dipolaritons

### A: Derivation of dynamic equations (lowest order of mean-field theory)

In the following section we present a derivation of Eqns. (3)–(5) which describe the dynamics of dipolariton system. For the macroscopic occupation of the modes one can treat fields as classical and calculate the dynamics of the system using mean value of their creation (or annihilation) operators. Using the Hamiltonian (1) and Master equation (2), one can write the equation of motion for mean value of operator $\hat{a}$ as

$$\hbar\partial_t\langle\hat{a}\rangle(t) = i\mathrm{Tr}\{\hat{a}[\rho,\hat{\mathcal{H}}_{coh}]\} = i\mathrm{Tr}\{\rho[\hat{\mathcal{H}}_{coh},\hat{a}]\}, \tag{10}$$

where we used the cyclic properties of the trace. The commutator in a RHS using explicit form of the Hamiltonian reads

$$\left[\omega_C\hat{a}^\dagger\hat{a} + \omega_{DX}\hat{b}^\dagger\hat{b} + \omega_{IX}\hat{c}^\dagger\hat{c} + \frac{\Omega}{2}(\hat{a}^\dagger\hat{b} + \hat{b}^\dagger\hat{a}) - \frac{J}{2}(\hat{b}^\dagger\hat{c} + \hat{c}^\dagger\hat{b}) + P\hat{a}^\dagger + P^*\hat{a}, \hat{a}\right], \tag{11}$$

and can be calculated part by part. Naturally, only first, fourth and penultimate terms contribute to the equation. Using standard commutation relations for bosons, one gets $\omega_C[\hat{a}^\dagger\hat{a},\hat{a}] = -\omega_C\hat{a}$, $\frac{\Omega}{2}[\hat{a}^\dagger\hat{b},\hat{a}] = -\frac{\Omega}{2}\hat{b}$, and $P[\hat{a}^\dagger,\hat{a}] = -P$. The coherent part of the equations for $\langle\hat{b}\rangle(t)$ and $\langle\hat{c}\rangle(t)$ can be written in the same way.

The incoherent processes can be treated using Lindblad superoperator [1]. In particular, the accounting of the life time of cavity mode can be included to the Eq. (10) as

$$\partial_t\langle\hat{a}\rangle(t) = \mathrm{Tr}\{\hat{a}\frac{\partial\rho(t)}{\partial t}\} = \mathrm{Tr}\{\hat{a}\frac{\gamma_C}{2}(2\hat{a}\rho\hat{a}^\dagger - \hat{a}^\dagger\hat{a}\rho - \rho\hat{a}^\dagger\hat{a})\}. \tag{12}$$

The first term gives $\gamma_C\mathrm{Tr}\{\rho\hat{a}^\dagger\hat{a}\hat{a}\} = \gamma_C\mathrm{Tr}\{\rho\hat{a}\hat{a}^\dagger\hat{a}\} - \gamma_C\mathrm{Tr}\{\rho\hat{a}\}$, where we used the relation $(\hat{a}^\dagger\hat{a})\hat{a} = \hat{a}(\hat{a}^\dagger\hat{a} - 1)$. The second term reads as $-\frac{\gamma_C}{2}\mathrm{Tr}\{\rho\hat{a}\hat{a}^\dagger\hat{a}\}$, and third term yields $-\frac{\gamma_C}{2}\mathrm{Tr}\{\rho\hat{a}^\dagger\hat{a}\hat{a}\} = -\frac{\gamma_C}{2}\mathrm{Tr}\{\rho\hat{a}\hat{a}^\dagger\hat{a}\} + \frac{\gamma_C}{2}\mathrm{Tr}\{\rho\hat{a}\}$. The summation of all terms results into incoherent part of dynamics in the form

$$\partial_t\langle\hat{a}\rangle(t) = -\frac{\gamma_C}{2}\langle\hat{a}\rangle. \tag{13}$$

The decoherent part of $\langle\hat{b}\rangle(t)$ and $\langle\hat{c}\rangle(t)$ can be derived in the same fashion, leading to the system of three coupled equations (3)–(5) in the main text which describes dipolariton system. An analogous system of equations can be derived from the three coupled oscillators Hamiltonian, which is shown in Section C.

### B: Derivation of dynamic equations (higher order of mean-field theory)

In the previous section we derived equations which describe dipolariton system in the lowest order of mean-field theory. Here we generalize it to the next order and derive equation for the occupation numbers of the modes correlators. In the following derivation we will treat coherent and incoherent processes separately.

*Coherent part.* We start from the Hamiltonian given by Eq. (1). The time dependence of the occupation numbers and correlators can be found using relation

$$\partial_t n_i(t) = \mathrm{Tr}\{\hat{a}_i^\dagger\hat{a}_i\partial_t\rho(t)\}, \tag{14}$$

where $\hat{a}_i$ represents operator of different type. The equation can be rewritten in the form

$$\partial_t n_i(t) = \frac{i}{\hbar}\mathrm{Tr}\{\hat{a}_i^\dagger\hat{a}_i[\rho,\hat{\mathcal{H}}_{coh}]\}, \tag{15}$$

and simplified using the explicit expression for coherent part of the Hamiltonian. To describe the dynamics we need to write system of six coupled equations for occupation numbers of the modes $n_C = \langle\hat{a}^\dagger\hat{a}\rangle$, $n_{DX} = \langle\hat{b}^\dagger\hat{b}\rangle$, $n_{IX} = \langle\hat{c}^\dagger\hat{c}\rangle$ and correlators $\alpha_{ab} = \langle\hat{a}^\dagger\hat{b}\rangle$, $\alpha_{bc} = \langle\hat{b}^\dagger\hat{c}\rangle$ and $\alpha_{ac} = \langle\hat{a}^\dagger\hat{c}\rangle$. Using mean-field approximation, we derive equation each type of occupation number and correlator. For instance, the occupation number of indirect excitons can be written as

$$\partial_t n_{IX}(t) = i\mathrm{Tr}\{\rho\left[\omega_C\hat{a}^\dagger\hat{a} + \omega_{DX}\hat{b}^\dagger\hat{b} + \omega_{IX}\hat{c}^\dagger\hat{c} + \frac{\Omega}{2}(\hat{a}^\dagger\hat{b} + \hat{b}^\dagger\hat{a}) - \frac{J}{2}(\hat{b}^\dagger\hat{c} + \hat{c}^\dagger\hat{b}), \hat{c}^\dagger\hat{c}\right]\}. \tag{16}$$

The first four terms of commutator are zero, while last term gives

$$-\frac{J}{2}\left(\left[\hat{b}^\dagger\hat{c},\hat{c}^\dagger\hat{c}\right]+\left[\hat{c}^\dagger\hat{b},\hat{c}^\dagger\hat{c}\right]\right)=-\frac{J}{2}\left([\hat{b}^\dagger\hat{c},\hat{c}^\dagger]\hat{c}+\hat{c}^\dagger[\hat{b}^\dagger\hat{c},\hat{c}]+[\hat{c}^\dagger\hat{b},\hat{c}^\dagger]\hat{c}+\hat{c}^\dagger[\hat{c}^\dagger\hat{b},\hat{c}]\right)=-\frac{J}{2}\left(\hat{b}^\dagger\hat{c}-\hat{c}^\dagger\hat{b}\right), \tag{17}$$

with final equation

$$\partial_t n_{IX}(t)=J\mathrm{Im}\alpha_{bc}, \tag{18}$$

where we used relation $\mathrm{Im}A=(A-A^*)/2i$. One can write equations for $n_C$ and $n_{DX}$ in the same fashion.

Derivation of dynamic equations for correlators require more efforts, but can be done straightforwardly. For example, the equation for correlator $\alpha_{ab}=\langle\hat{a}^\dagger\hat{b}\rangle$ reads as

$$\partial_t\alpha_{ab}(t)=i\mathrm{Tr}\{\rho\left[\omega_C\hat{a}^\dagger\hat{a}+\omega_{DX}\hat{b}^\dagger\hat{b}+\omega_{IX}\hat{c}^\dagger\hat{c}+\frac{\Omega}{2}\hat{a}^\dagger\hat{b}+\frac{\Omega}{2}\hat{b}^\dagger\hat{a}-\frac{J}{2}\hat{b}^\dagger\hat{c}+\frac{J}{2}\hat{c}^\dagger\hat{b},\hat{a}^\dagger\hat{b}\right]\}. \tag{19}$$

Considering terms one by one, the first gives $\omega_C[\hat{a}^\dagger\hat{a},\hat{a}^\dagger\hat{b}]=\omega_C\hat{b}\hat{a}^\dagger$ and second term yields $\omega_{DX}[\hat{b}^\dagger\hat{b},\hat{a}^\dagger\hat{b}]=-\omega_{DX}\hat{a}^\dagger\hat{b}$. Naturally, third and forth terms give zero, while the fifth term is equal to $\Omega/2[\hat{a}\hat{b}^\dagger,\hat{a}^\dagger\hat{b}]=-\Omega/2(\hat{a}^\dagger\hat{a}-\hat{b}^\dagger\hat{b})$. The sixth term reads $-J/2[\hat{b}^\dagger\hat{c},\hat{a}^\dagger\hat{b}]=J/2\ \hat{a}^\dagger\hat{c}$, and last term from correlator in Eq. (19) is zero. It is convenient to perform the same analysis for correlator $\langle\hat{a}\hat{b}^\dagger\rangle\equiv\alpha^*_{ab}$, and combine both expressions. This leads to dynamic equation for the real part of the correlator

$$\partial_t\mathrm{Re}\alpha_{ab}(t)=(\omega_{DX}-\omega_C)\mathrm{Im}\alpha_{ab}-\frac{J}{2}\mathrm{Im}\alpha_{ac}, \tag{20}$$

where relation $\mathrm{Re}A=(A+A^*)/2$ was used. Equations for $\partial_t\alpha_{bc}$ and $\partial_t\alpha_{ac}$ can be derived analogously.

Finally, assuming the presence of coherent pump, we need to add three equation for $\langle\hat{a}\rangle$, $\langle\hat{b}\rangle$ and $\langle\hat{c}\rangle$ given by Eqns. (3)–(5) in the main text of the article. This leads to complete system of Eqns. (28)–(36) for dynamics of dipolariton system written in the end of the section.

*Decoherent part.* The Master equation for density matrix is a powerful tool which allows one to account for various incoherent processes. It can be introduced in the model using Lindblad superoperator. In particular, the effect of temperature can be modelled using phonon bath with chosen Bose distribution function, as was done in Refs. [1] and [2]. In the following considerations we do not consider $k$-space dynamics of the system and energy relaxation of dipolariton modes. However, we do need to account for dissipation processes coming from leakage of cavity mode out of the mirrors, as well as radiative and non-radiative recombination of excitons.

*Dissipation processes* can be modelled with Lindblad superoperator written for any operator $\hat{a}_i$ of type $i$ in the form

$$\hat{\mathcal{L}}_{dis}\rho=i\frac{\Gamma_i}{2}\left(2\hat{a}\rho\hat{a}^\dagger-\hat{a}^\dagger\hat{a}\rho-\rho\hat{a}^\dagger\hat{a}\right), \tag{21}$$

where $\Gamma_i=\hbar\gamma_i$ represent the decay rate of the mode, $i=C,DX,IX$. Reminding the Master equation, $i\hbar\frac{\partial\rho}{\partial t}=[\hat{\mathcal{H}},\rho]+\hat{\mathcal{L}}\rho$, one can write the incoherent part of dynamic equation for occupation numbers and correlators. For instance, in the case of cavity photon occupancy it reads

$$\partial_t n_C(t)=\mathrm{Tr}\{\hat{a}^\dagger\hat{a}\frac{\partial\rho(t)}{\partial t}\}=\mathrm{Tr}\{\hat{a}^\dagger\hat{a}\frac{\gamma_C}{2}(2\hat{a}\rho\hat{a}^\dagger-\hat{a}^\dagger\hat{a}\rho-\rho\hat{a}^\dagger\hat{a})\}=\gamma_C\mathrm{Tr}\{\rho(\hat{a}^\dagger\hat{a}^\dagger\hat{a}\hat{a}-\hat{a}^\dagger\hat{a}\hat{a}^\dagger\hat{a})\}, \tag{22}$$

where to write the latter expression we used the cyclic properties of the trace. Applying the mean-field approximation, $\langle\hat{n}_C\rangle=\langle\hat{a}^\dagger\hat{a}\rangle=\mathrm{Tr}\{\hat{n}_C\rho\}$ and $\langle\hat{a}^\dagger\hat{a}^\dagger\hat{a}\hat{a}\rangle=\mathrm{Tr}\{\hat{n}_C(\hat{n}_C-1)\rho\}$, it can be rewritten as

$$\partial_t n_C(t)=\gamma_C\mathrm{Tr}\{\rho(\hat{n}_C(\hat{n}_C-1)-\hat{n}_C^2)\}=-\gamma_C n_C. \tag{23}$$

The same considerations are valid for $\partial_t n_{DX}(t)$, $\partial_t n_{IX}(t)$ and correlators.

The lifetime of the mode is not the only cause which affects dynamics of the system. Indeed, the coherence in the system can be spoiled due to dephasing even for infinitely long-lived atomic systems. There the main effect of loosing coherence can be introduced by *pure decoherence* term, which acts solely on off-diagonal terms or "coherences", while live diagonal terms are unaffected. Usually written for two-level system (atom, qubit etc), the Lindblad operator for pure coherence in general form reads [3]

$$\hat{\mathcal{L}}_{dec}\rho=-i\Gamma^{(dec)}\left[\sigma_z,[\sigma_z,\rho]\right], \tag{24}$$

where $\sigma_z = [\sigma^\dagger, \sigma]/2$, $\sigma^\dagger$ is a fermionic creation operator, and $\Gamma^{(dec)}$ denotes rate of pure dephasing. In particular, for two-level system it thus can be rewritten as $\hat{\mathcal{L}}_{dec}\rho = i\frac{\Gamma^{(dec)}}{2}(\sigma_z\rho\sigma_z - \rho)$ [4]. In our system we want to account for decay of coherence of the interaction between different modes which have bosonic statistics. Therefore, we can map angular momentum operators into bosonic operators using Holstein-Primakoff transformations [5], $\sigma_z = (s - \hat{a}^\dagger\hat{a})$, where $s = 1$ is spin of the particle. Then Lindblad operator (24) can be rewritten opening the commutator and reads

$$\hat{\mathcal{L}}_{dec}\rho = i\Gamma^{(dec)}\left(2\hat{a}^\dagger\hat{a}\rho\hat{a}^\dagger\hat{a} - \hat{a}^\dagger\hat{a}\hat{a}^\dagger\hat{a}\rho - \rho\hat{a}^\dagger\hat{a}\hat{a}^\dagger\hat{a}\right). \tag{25}$$

Plugging (25) into equation for occupation number

$$\partial_t n_C(t) = \gamma^{(dec)}\mathrm{Tr}\{\hat{a}^\dagger\hat{a}\left(2\hat{a}^\dagger\hat{a}\rho\hat{a}^\dagger\hat{a} - \hat{a}^\dagger\hat{a}\hat{a}^\dagger\hat{a}\rho - \rho\hat{a}^\dagger\hat{a}\hat{a}^\dagger\hat{a}\right)\} = 0 \tag{26}$$

one can check that it gives zero contribution to the lifetime of the mode. Performing the same analysis for correlator (e. g. $\alpha_{ab}$) we straightforwardly derive

$$\partial_t\alpha_{ab}(t) = \gamma_{ab}^{(dec)}\mathrm{Tr}\{\hat{a}^\dagger\hat{b}\left(2\hat{a}^\dagger\hat{a}\rho\hat{a}^\dagger\hat{a} - \hat{a}^\dagger\hat{a}\hat{a}^\dagger\hat{a}\rho - \rho\hat{a}^\dagger\hat{a}\hat{a}^\dagger\hat{a}\right)\} = \gamma_{ab}^{(dec)}\mathrm{Tr}\{\rho\hat{a}^\dagger\hat{b}(2\hat{a}\hat{a}^\dagger\hat{a}^\dagger\hat{a} - \hat{a}^\dagger\hat{a}\hat{a}^\dagger\hat{a} - \hat{a}\hat{a}^\dagger\hat{a}\hat{a}^\dagger)\} = -\gamma_{ab}^{(dec)}\langle\hat{a}^\dagger\hat{b}\rangle. \tag{27}$$

Thus, coherence between mode is destroyed for large damping rates $\gamma_{ab}^{dec}$, and index corresponds to the type of correlator we are interested in. Similarly, one introduce pure decoherence for $\alpha_{bc}$ and $\alpha_{ac}$ correlators.

Finally, merging coherent and decoherent parts, we come to the system of equations

$$\partial n_C/\partial t = \Omega\mathrm{Im}\alpha_{ab} - \gamma_C n_C - 2\mathrm{Im}\{\widetilde{P}^*\langle\hat{a}\rangle\}, \tag{28}$$

$$\partial n_{DX}/\partial t = -\Omega\mathrm{Im}\alpha_{ab} - J\mathrm{Im}\alpha_{bc} - \gamma_{DX}n_{DX}, \tag{29}$$

$$\partial n_{IX}/\partial t = J\mathrm{Im}\alpha_{bc} - \gamma n_{IX}, \tag{30}$$

$$\frac{\partial(\mathrm{Re}\alpha_{ab})}{\partial t} = -\delta_\Omega\mathrm{Im}\alpha_{ab} - \frac{J}{2}\mathrm{Im}\alpha_{ac} - \frac{\gamma_{ab}}{2}\mathrm{Re}\alpha_{ab} - \gamma_{ab}^{(dec)}\mathrm{Re}\alpha_{ab} - \mathrm{Im}\{\widetilde{P}^*\langle\hat{b}\rangle\}, \tag{31}$$

$$\frac{\partial(\mathrm{Re}\alpha_{bc})}{\partial t} = \delta_J\mathrm{Im}\alpha_{bc} - \frac{\Omega}{2}\mathrm{Im}\alpha_{ac} - \frac{\gamma_{bc}}{2}\mathrm{Re}\alpha_{bc} - \gamma_{bc}^{(dec)}\mathrm{Re}\alpha_{bc}, \tag{32}$$

$$\frac{\partial(\mathrm{Re}\alpha_{ac})}{\partial t} = -(\delta_\Omega - \delta_J)\mathrm{Im}\alpha_{ac} - \frac{J}{2}\mathrm{Im}\alpha_{ab} + \frac{\Omega}{2}\mathrm{Im}\alpha_{bc} - \frac{\gamma_{ac}}{2}\mathrm{Re}\alpha_{ac} - \gamma_{ac}^{(dec)}\mathrm{Re}\alpha_{ac} - \mathrm{Im}\{\widetilde{P}^*\langle\hat{c}\rangle\}, \tag{33}$$

$$\partial\langle\hat{a}\rangle/\partial t = -i\Omega/2\langle\hat{b}\rangle - \gamma_C/2\langle\hat{a}\rangle - i\widetilde{P}, \tag{34}$$

$$\partial\langle\hat{b}\rangle/\partial t = i\delta_\Omega\langle\hat{b}\rangle - iJ/2\langle\hat{c}\rangle - i\Omega/2\langle\hat{a}\rangle - \gamma_{DX}/2\langle\hat{b}\rangle, \tag{35}$$

$$\partial\langle\hat{c}\rangle/\partial t = i(\delta_\Omega - \delta_J)\langle\hat{c}\rangle - iJ/2\langle\hat{b}\rangle - \gamma_{IX}/2\langle\hat{c}\rangle, \tag{36}$$

where $\gamma_{ab} = \gamma_C + \gamma_{DX}$, $\gamma_{bc} = \gamma_{DX} + \gamma_{IX}$ and $\gamma_{ac} = \gamma_C + \gamma_{IX}$ are reduced damping constants used in correlators.

Additionally, we introduced terms corresponding to pure decoherence to the correlators, with rates being $\gamma_{ab}^{(dec)}$, $\gamma_{bc}^{(dec)}$ and $\gamma_{ac}^{(dec)}$. This allows to account temperature effects and other incoherent processes.

The numerical calculation for dynamics of the modes $n_{IX}(t)$ and $n_{DX}(t)$ calculated using system of Eqns. (3)–(5) written in the main text and advanced system (28)–(36) presented above give the same result for the chosen pumping conditions, and thus ensures the validity of used mean field approximation. Therefore, while the model formulated in Section B is rather general, we do not use it for calculations and leave the problem of accounting of decoherent processes for future works.

### C: Simplified model

Here we present model based on the simple three coupled oscillators Hamiltonian used in Ref. [8]. The Hamiltonian and corresponding wave function read

$$H = \hbar\begin{pmatrix} \omega_{IX} & -J/2 & 0 \\ -J/2 & \omega_{DX} & \Omega/2 \\ 0 & \Omega/2 & \omega_C \end{pmatrix},\ |\Psi\rangle = \begin{pmatrix} \Psi_{IX} \\ \Psi_{DX} \\ \Psi_C \end{pmatrix}, \tag{37}$$

where the wave-function $|\Psi\rangle$ of a dipolariton can be expanded in the basis of uncoupled states $\Psi_C$, $\Psi_{DX}$ and $\Psi_{IX}$ being field operators for cavity photon, direct exciton and indirect exciton, respectively. Here we essentially assume

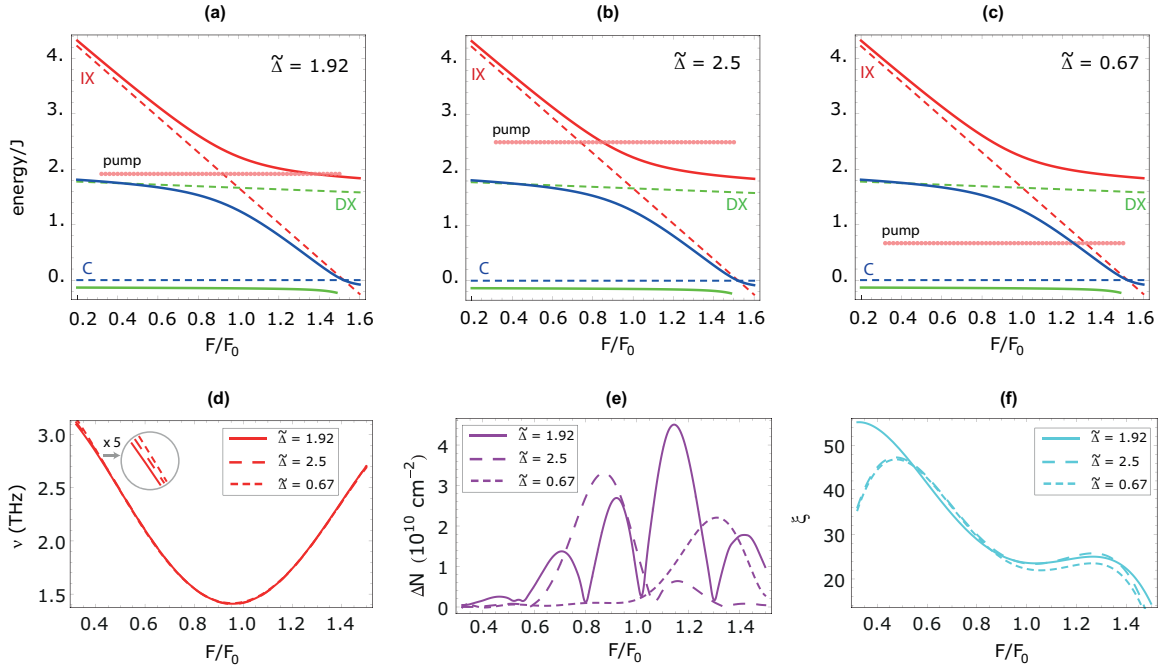


FIG. 4: (Color online) (a), (b) and (c): Energy spectrum of dipolariton modes (solid lines) as a function of normalized electric field $F/F_0$ plotted for $\delta_\Omega = -1.67$. We assume equal IX-DX and C-DX coupling constants, measure energy in units of $J$ and choose cavity mode as a reference point, $E_C = 0$. Pink dotted lines show energy position of the pumping of the cavity mode. (d) Frequency of long-term indirect exciton density oscillations $\nu$ for different electric field, showing the possible tunable window of the signal frequency. Tunnelling frequency used for calculations is $J/2\pi = 1.45$ THz. (e) Amplitude of oscillations showing the correspondence between pumping conditions and mode detuning. (e) Quality factor of the oscillations defined as ratio between amplitude and decrement of oscillation.

macroscopic occupation numbers for each mode, which allows us to use mean-field description and treat $\Psi_C$, $\Psi_{DX}$ and $\Psi_{IX}$ as classical fields. This enables describing the dynamics of the system by a closed set of time-dependent Schrödinger equations. To separate the rapidly oscillating part of dynamics we adopt the rotating frame using transformations: $\Psi_{IX}(t) = \psi_{IX}(t)e^{-i\omega_{IX}t}$, $\Psi_{DX}(t) = \psi_{DX}(t)e^{-i\omega_{DX}t}$ and $\Psi_C(t) = \psi_C(t)e^{-i\omega_C t}$ [6]. Finally, the system of equations describing dynamics of dipolariton system on a mean-field level reads

$$\frac{\partial\psi_{IX}(t)}{\partial t} = i\frac{J}{2}\psi_{DX}(t)e^{i\delta_J t} - \frac{\gamma_{IX}}{2}\psi_{IX}(t), \tag{38}$$

$$\frac{\partial\psi_{DX}(t)}{\partial t} = i\frac{J}{2}\psi_{IX}(t)e^{-i\delta_J t} - i\frac{\Omega}{2}\psi_C(t)e^{-i\delta_\Omega t} - i\frac{\gamma_{DX}}{2}\psi_{DX}(t), \tag{39}$$

$$\frac{\partial\psi_C(t)}{\partial t} = -i\frac{\Omega}{2}\psi_{DX}(t)e^{i\delta_\Omega t} - iP_0(t)e^{-i\Delta t} - \frac{\gamma_C}{2}\psi_C(t), \tag{40}$$

where the photonic detuning $\delta_\Omega = \omega_C - \omega_{DX}$ for the cavity photon coupled to the direct exciton, and energy distance between spatially indirect and direct excitons $\delta_J = \omega_{IX} - \omega_{DX}$ were introduced. The frequency of the resonant optical pumping $P_0(t)$ is detuned from the photon mode by $\Delta = \omega_P - \omega_C$ (second term in RHS of Eq. (38)).

The presented description has shown to be well-suitable in numerous works devoted to physics of exciton-polaritons. However, it has serious drawback since does not account for decoherence in the real systems. The dissipation though can introduced in the system in phenomenological way, as we did adding last terms in Eqns. (38). They are proportional to damping rates for each mode $\gamma_i = 2\pi/\tau_i$, $i = C,\ DX,\ IX$. The lifetimes of the modes being typically $\tau_C \approx 3$ ps, $\tau_{DX} \approx 1$ ns and $\tau_{IX} \approx 100$ ns. In the case where decoherence plays substantial role in the dipolariton system, this approach is not valid and one has to use the model from Section A based on the Master equation.

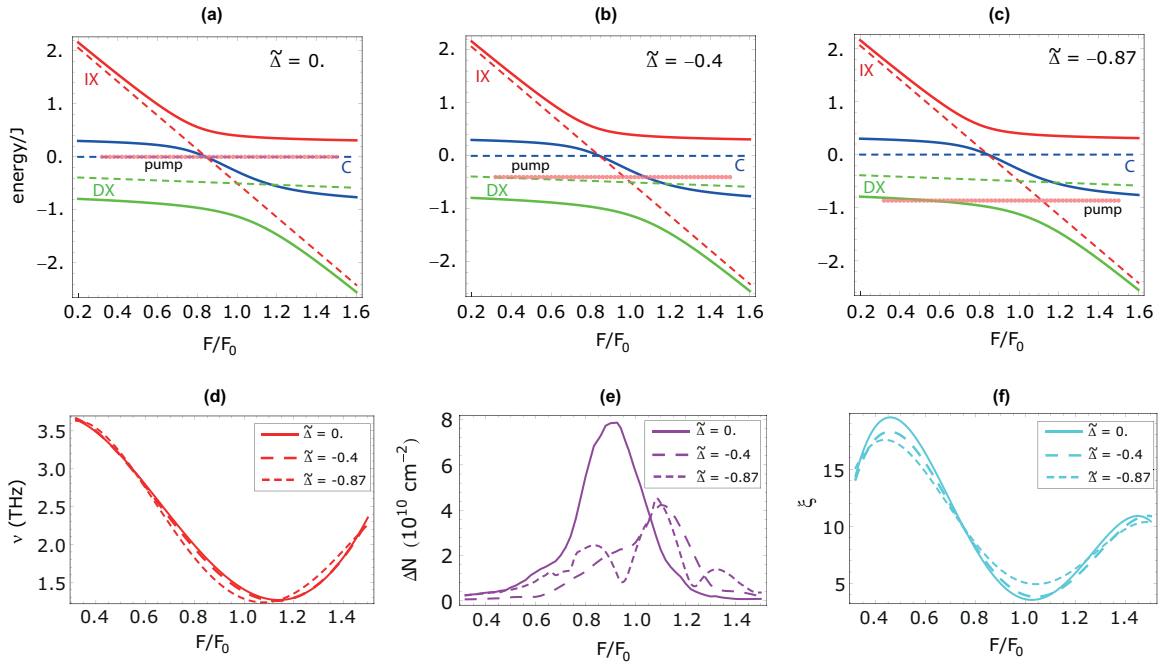


FIG. 5: (Color online) (a), (b) and (c): Energy spectrum of dipolariton modes (solid lines) as a function of normalized electric field $F/F_0$ plotted for $\delta_\Omega = 0.5$. Pink dotted lines show energy position of the pumping of the cavity mode. (d) Frequency of long-term indirect exciton density oscillations $\nu$ for different electric field, showing the range where signal frequency can be tuned. (e) Amplitude of oscillations showing the correspondence between pumping conditions and mode detuning. (e) Quality factor of the oscillations defined as ratio between amplitude and decrement of oscillation.

### D: Dynamics analysis

In the work we have studied the dynamics of indirect exciton density oscillations which induce emission of coherent THz radiation. These oscillations emerge due to the strong coupling between three modes, namely: indirect excitons (IX), direct excitons (DX) and cavity photons (C). In general, the dynamics of dipolaritons described by system of coupled equations for occupation numbers and correlators is complex due to the presence of mixing terms, detuning, decay and tunable pumping conditions. It can be described by characteristic energies $\hbar J$ and $\hbar\Omega$ which denote IX-DX and C-DX coupling, respectively, detuning parameters $\delta_J = \omega_{IX} - \omega_{DX}$ and $\delta_\Omega = \omega_C - \omega_{DX}$, and pumping frequency detuning from the cavity mode $\Delta = \omega_P - \omega_C$. Consequently, in order to comprehend the dynamics of the system one needs to study the dependence of density oscillations on five independent parameters, which is a non-trivial task.

The coupling constants of light-matter interaction $\hbar\Omega$ and indirect exciton to direct exciton coupling $\hbar J$ are intrinsic characteristics of the structure. The structure can be designed in such a way that these two characteristics coincide: $\hbar\Omega = \hbar J$, in which case DX, IX and C modes are efficiently intermixed. This regime has already been studied in the samples where dipolariton modes have been observed for the first time [7, 8] with $\hbar\Omega = \hbar J = 6$ meV. Therefore, the behavior of dipolaritons can be controlled tuning the energy spacing between modes by altering the applied electric field ($\delta_J$) and tuning the incidence angle of the excitation light ($\delta_\Omega$).

We shall specifically consider two particular cases. In the first case the cavity mode is far detuned from the IX-DX resonance, which partially resembles the weak light-matter coupling (regime $I$). The second case refers to the resonance of all three modes achieved for a certain incidence angle where $\delta_\Omega$ is small (regime $II$). For each regime we study the dependence of properties of indirect exciton density oscillations on the applied voltage. To keep the results general, the analysis is performed in dimensionless units $F/F_0$, where electric field is normalized to value where IX and DX resonances anti-cross, $F_0$. Moreover, we measure the frequency in units of tunnelling coupling $J$. Finally, the last parameter which governs the dynamics of the system is the pumping frequency $\omega_P = \Delta + \omega_C$.

In the main text of this paper we present the plot of indirect indirect exciton density oscillations for two particular situations (Fig. 2 in the main text). In general case the dynamics exhibits turning-on transitional region lasting for several picoseconds after the arrival of the pulse followed by subsequent long-term oscillations of density decaying in time. Here we vary the pumping conditions and study the "quality" of oscillations. To do this we use the following

set of parameters. Complementary to the frequency of long-range oscillations, we find the averaged amplitude of the oscillations in transient regime $\Delta N$ to define the efficiency of pumping conditions. This quantity strongly affects the power output of generated initial THz signal and it is important for achievement of powerful pulsed THz emission. Additionally, we define dimensionless oscillation quality factor $\xi$ defined as a ratio of long-term oscillation amplitude $\Delta N$ to its decrement in time $\delta N$. Therefore, high $\xi$ stands for slowly decaying oscillations with comparably large amplitude.

We consider the first regime when cavity mode is far-detuned from the IX-DX anti-crossing region, $\delta_\Omega = -1.67$. In energy diagrams in Fig. 4(a,b,c) we chose three pumping energies corresponding to the resonant pumping ($\Delta = 1.92$), blue detuned pumping ($\Delta = 2.5$) and red-detuned pumping ($\Delta = -0.67$). Solid lines there denote upper, middle and lower dipolariton branches (red, blue and green lines, respectively). The energy is counted from the bottom of the cavity mode ($E_C = 0$). Fig. 4(d) shows dependence of the frequency of $n_{IX}$ oscillations as function of the electric field for different pumping energy shown in energy diagrams in Fig. 4(a,b,c) (pink line). One can see that it has the minimum value for almost resonant electric field $F/F_0 \approx 0.9$ and approximately corresponds to tunnelling coupling $\nu \approx J/2\pi = 1.45$ THz. Also, it increases with the increase of detuning between IX and DX modes, $\delta_J$. Moreover, we note that the frequency of stabilized oscillations does not depend on the pumping conditions. In Fig. 4(e) we show amplitude of oscillations. It differs drastically for three pumping frequencies. One can see that $\Delta N$ increases if pump coincides with energy bare transition or dipolariton mode, and this correlation can be tracked in Fig. 4(e) for all detunings. However, calculations show that oscillations with the largest amplitude correspond to the strongest decrement of oscillations, which result into minimal $\xi$ in the resonant region (Fig. 4(f)). Out of the resonance both amplitude oscillation and decay are small, and the realistic region should be chosen between electric field corresponding to maxima of the quality factor $\xi$.

Next, we study the second regime where cavity mode is detuned from direct exciton by $\delta_\Omega = 0.5$. In the IX-DX resonance point dipolariton represents strong mixture of bare modes with two anti-crossings shown in Fig. 4(a-c). The dynamics of the system was calculated for three pumping energies which change from resonance (Fig. 4(a), $\Delta = 0$) to out-of-resonance conditions (Fig. 4(c), $\Delta = -0.87$). Fig. 5(d) shows no influence of pumping conditions on the oscillation frequency, while the position of the minimum shifts to $F/F_0 \approx 1.1$ point. An amplitude of oscillations in Fig. 5(e) shows the same correlation with respect to pumping conditions observed in the first regime, while its absolute value is larger. However, the quality factor $\xi$ of oscillation in second regime is several times lower due to faster decay of oscillations (Fig. 5(f)).

Thus, we can conclude that the first regime is appropriate for the cases where stable long-term emission of THz radiation is required, while the second regime is needed for the pulsed generation of powerful signals.

### E: Sketch of system with supplemental THz cavity

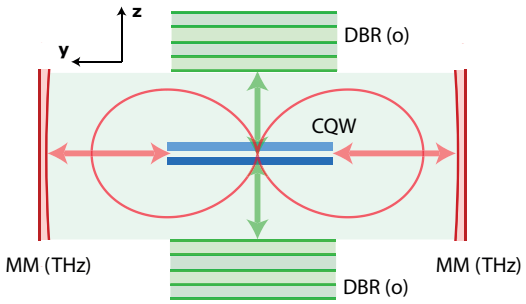


FIG. 6: (Color online) Sketch of the geometry where power of THz emission is increased due to Purcell effect (top view). Here DBR (o) represent optical cavity mirrors (green), while MM (THz) denote metallic mirror cavity tuned to reflect signal of THz frequency (red). The red lines show peculiar polar pattern of dipolariton THz emitter.

[1] I. G. Savenko, I. A. Shelykh, and M. A. Kaliteevski, Phys. Rev. Lett. **107**, 027401 (2011).
[2] A. V. Kavokin, I. A. Shelykh, T. Taylor, and M. M. Glazov, Phys. Rev. Lett. **108**, 197401 (2012).

[3] M. A. Schlosshauer, *Decoherence and the Quantum-to-Classical Transition* (Springer, Berlin, 2007).
[4] A. Gonzalez-Tudela, E. Del Valle, E. Cancellieri, C. Tejedor, D. Sanvitto, F. P. Laussy, Optics Express **18**, 7002 (2010).
[5] T. Holstein and H. Primakoff, Phys. Rev. **58**, 1098 (1940).
[6] A. V. Kavokin, J. J. Baumberg, G. Malpuech, and F. P. Laussy, *Microcavities* (Oxford University Press, Oxford, 2007).
[7] G. Christmann, A. Askitopoulos, G. Deligeorgis, Z. Hatzopoulos, S. I. Tsintzos, P. G. Savvidis, and J. J. Baumberg, Appl. Phys. Lett. **98**, 081111 (2011).
[8] P. Cristofolini, G. Christmann, S. I. Tsintzos, G. Deligeorgis, G. Konstantinidis, Z. Hatzopoulos, P. G. Savvidis, and J. J. Baumberg, Science **336**, 704 (2012).